NANO LETTERS

Letter

pubs.acs.org/NanoLett

High-Density Nanosharp Microstructures Enable Efficient CO_2 Electroreduction

Tina Saberi Safaei,[†] Adam Mepham,[‡] Xueli Zheng,[†,§] Yuanjie Pang,[∥] Cao-Thang Dinh,[†] Min Liu,[†] David Sinton,[∥] Shana O. Kelley,[*,‡,⊥,#] and Edward H. Sargent[*,†]

[†]Department of Electrical and Computer Engineering, University of Toronto, 35 St George Street, Toronto, Ontario M5S 1A4, Canada

[‡]Institute for Biomaterials and Biomedical Engineering, University of Toronto, 164 College Street, Toronto, Ontario M5S 3G9, Canada

[§]Tianjin Key Laboratory of Composite and Functional Materials, School of Materials Science and Engineering, Tianjin University, Tianjin 300072, China

[∥]Department of Mechanical and Industrial Engineering, University of Toronto, 5 King's College Road, Toronto, Ontario M5S 3G8, Canada

[⊥]Department of Pharmaceutical Sciences, Leslie Dan Faculty of Pharmacy, University of Toronto, Toronto, Ontario M5S 3M2, Canada

[#]Department of Biochemistry, Faculty of Medicine, University of Toronto, 1 King's College Circle, Toronto, Ontario M5S 1A8, Canada

Supporting Information

ABSTRACT: Conversion of CO_2 to CO powered by renewable electricity not only reduces CO_2 pollution but also is a means to store renewable energy via chemical production of fuels from CO. However, the kinetics of this reaction are slow due its large energetic barrier. We have recently reported CO_2 reduction that is considerably enhanced via local electric field concentration at the tips of sharp gold nanostructures. The high local electric field enhances CO_2 concentration at the catalytic active sites, lowering the activation barrier. Here we engineer the nucleation and growth of next-generation Au nanostructures. The electroplating overpotential was manipulated to generate an appreciably increased density of honed nanoneedles. Using this approach, we report the first application of sequential electrodeposition to increase the density of sharp tips in CO_2 electroreduction. Selective regions of the primary nanoneedles are passivated using a thiol SAM (self-assembled monolayer), and then growth is concentrated atop the uncovered high-energy planes, providing new nucleation sites that ultimately lead to an increase in the density of the nanosharp structures. The two-step process leads to a new record in CO_2 to CO reduction, with a geometric current density of 38 mA/cm^2 at −0.4 V (vs reversible hydrogen electrode), and a 15-fold improvement over the best prior reports of electrochemical surface area (ECSA) normalized current density.

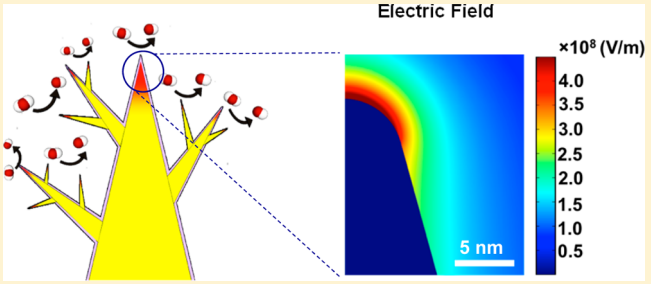

KEYWORDS: *CO_2 electroreduction, catalysis, gold nanoneedles, electroplating*

Electrochemical reduction of CO_2 to CO using electricity offers a means to store the abundant but intermittent energy available from renewable energy sources.[1−3] However, electrochemical conversion of CO_2 to valuable products suffers from slow kinetics, the need for high overpotentials, and poor product selectivity.[4,5] For example, the highly selective reduction of CO_2 to CO has been achieved with Au nanoparticles; however, the current density of the reaction was limited to only 2 mA/cm^2 at an overpotential of 0.24 V.[6] Several approaches including alloying,[7] shape control,[2,6,8] and surface functionalization[9,10] have been used to improve the performance of CO_2 to CO catalysts. Nevertheless, current densities have, until recently, remained below 3 mA/cm^2 at an applied voltage of −0.35 V relative to the reversible hydrogen electrode (RHE).

We recently reported the use of field-induced reagent concentration (FIRC) to achieve a high intensity of efficient CO_2 reduction.[11] The high local electric field at the sharp tips of metal nanostructures concentrates cation-complexed CO_2 molecules near the active surface of the catalyst (Figure 1a).[12,13] The Au nanoneedle electrodes exhibit CO_2 reduction with a

Received: August 27, 2016
Revised: October 6, 2016

DOI: 10.1021/acs.nanolett.6b03615
Nano Lett. XXXX, XXX, XXX−XXX

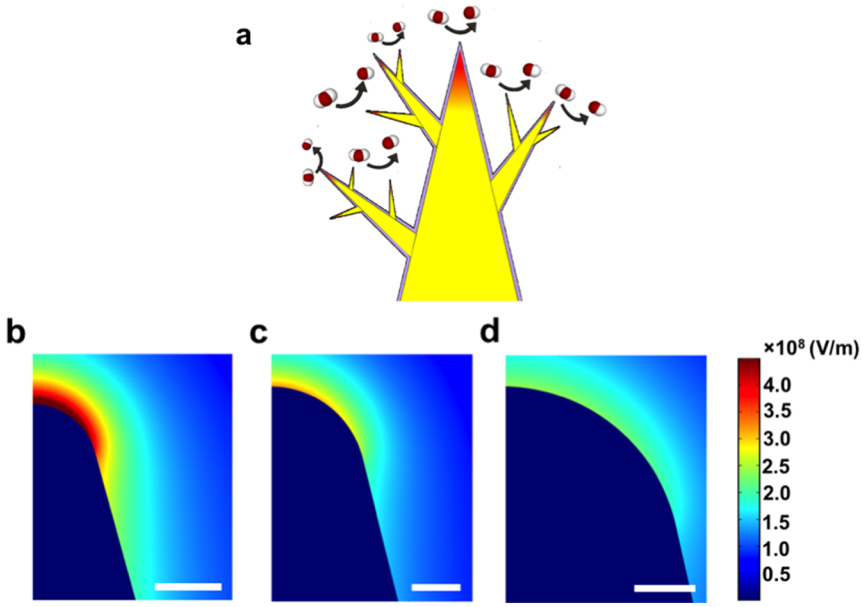

Figure 1. (a) Schematic of the multitip sharp Au nanoneedles with an increased number of active sites (higher density of tips). Finite element computation results showing the effect of nanoneedle tip radii of (b) 5 nm, (c) 10 nm, and (d) 15 nm on electric field concentration (the scale bars are 5 nm). A lower tip radius generates a higher electric field concentration.

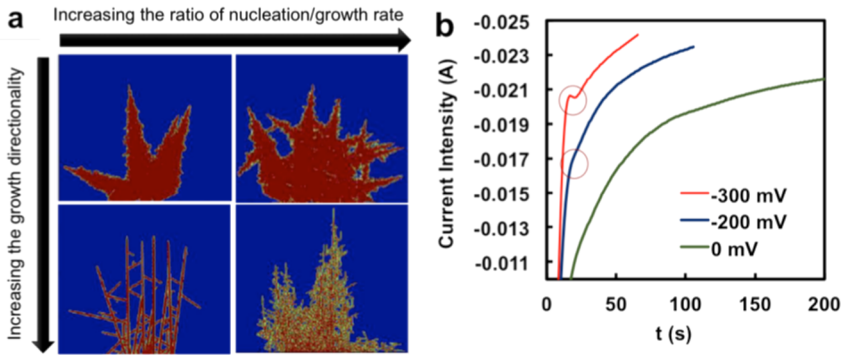

Figure 2. Higher plating overpotentials generate finer structures. (a) Modeling outcome demonstrates the growth of finer structures by increasing the nucleation/growth rate ratio and growth directionality. (b) A peak in current traces is observed at higher plating overpotentials, indicating the occurrence of a high degree of nucleation.

record-high geometric current density (j_{CO}) of 15 mA/cm^2 at the low potential of −0.35 V (η_{CO} = 0.24 V) with near quantitative Faradaic efficiencies (>95%). The electrochemical surface area (ECSA) normalized current density at −0.4 V, which reaches a value of 0.66 mA/cm^2, is over 30 times higher than for conventional nanorods and nanoparticles. We demonstrated that this enhancement in CO_2 reduction reaction rate is due to the locally concentrated electric field at the sharp tips of metal nanostructures and not because of the faceting of nanoneedles.

We began the present study by exploring the connection between the radius of curvature of nanostructured electrode tips and high local field using electrochemical simulation (Figure 1b). When we lowered the tip radius from 15 to 5 nm, for example, the electric field at the tip increased 2-fold. We focused on nanoneedles, since they allow for a higher degree of nanostructuring and accessibility to electrolyte, compared to other nanostructures such as nanoparticles and nanowires with a similar tip radius of curvature.

We focused on bottom-up fabrication of gold microstructures using electrodeposition on an insulator-passivated gold substrate onto which we had patterned apertures 15 μm in diameter.[14,15] The modeling output demonstrates that, by controlling the ratio of nucleation rate to growth rate (α) and also by controlling the growth directionality, finer structures can be formed (Figure 2a).

We sought therefore to manipulate, experimentally, the overpotential with the goal of controlling these parameters.[16] Higher overpotentials promote a surge in nucleation (higher α), which is evident from the peak in current observed after 15 s of deposition. Additionally, at high plating current densities, dendritic growth is favored: it overcomes the insufficient availability of reagents by concentrating the ionic replenishment at the growing tips of the structures. When we grow with a high α, severe local reagent depletion (resulting in the subsequent dip in current) promotes highly directional growth of gold structures into the bulk electrolyte.[17−19]

With lower α and lower plating currents, gold ions consumed in electrodeposition are efficiently replenished via diffusion. In this case, gold structures tend to grow in both the longitudinal and lateral directions and exhibit much more isotropic features (Figure 2b).[20]

DOI: 10.1021/acs.nanolett.6b03615
Nano Lett. XXXX, XXX, XXX−XXX

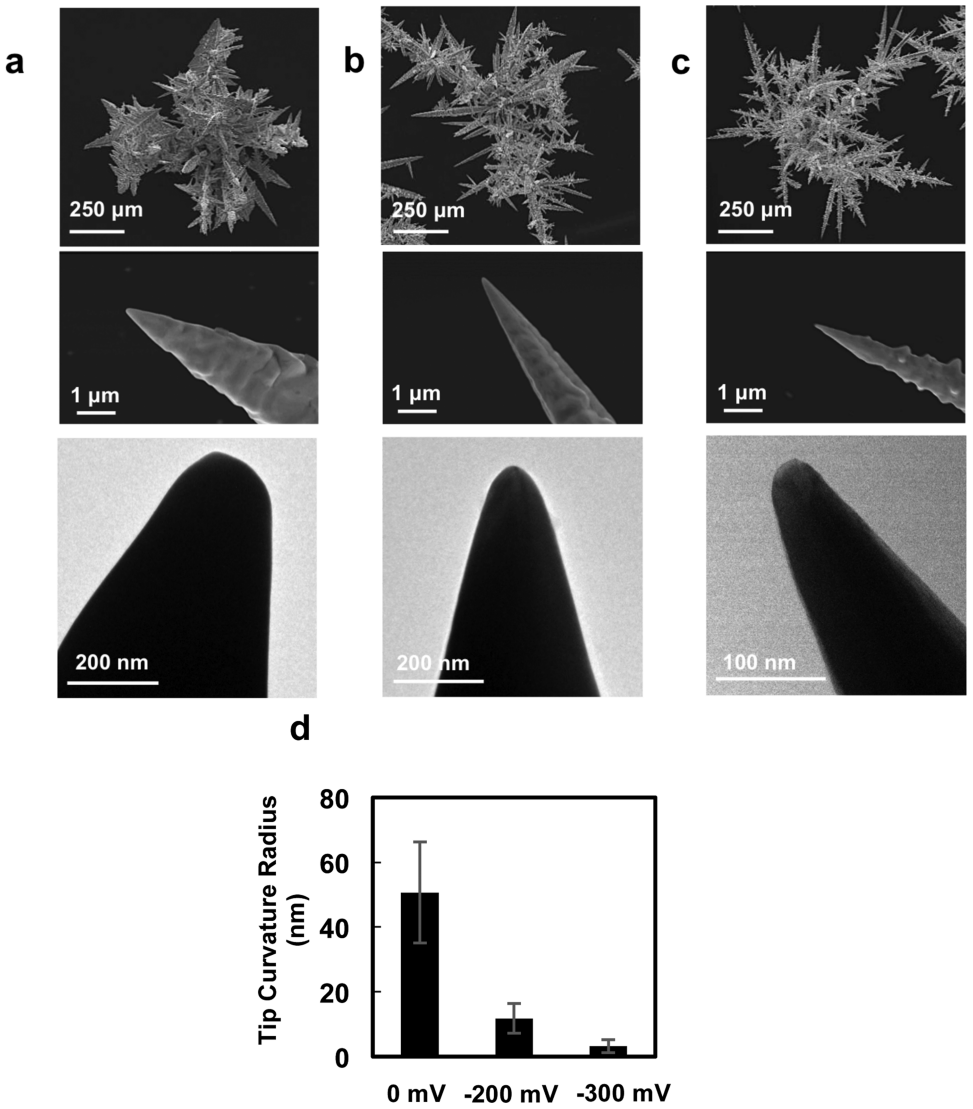

Figure 3. Higher overpotentials generate gold nanoneedles with lower tip radii of curvature. Electron microscopy images of gold structures grown at (a) 0 mV, (b) −200 mV, and (c) −300 mV. (d) Tip curvature radii measured from TEM images of nanoneedles deposited at different potentials.

Gold structures are electrodeposited from a solution of 450 mM $HAuCl_4$ in 0.5 mM HCl at 0, −0.2, and −0.3 V against an Ag/AgCl reference electrode. Electron microscopy images indicate that higher overpotentials promote directional growth and finer structures (Figure 3). As we decrease the overpotential, nanoneedles become coarser, and leaf-like structures start to appear (at 0 V). Based on the acquired TEM images, finer structures also have sharper tips. The measured tip radii of nanoneedles are 50, 12, and 3 nm at 0, −0.2, and −0.3 V respectively (Figure 3d).

To investigate the effect of sharpness on CO_2 reduction efficiency, we performed the reaction in CO_2-saturated 0.5 M $KHCO_3$ (pH 7.2) and analyzed the products using gas chromatography. Cyclic voltammetry experiments yielded higher current densities for the sharper structures, verifying faster kinetics for the CO_2 reduction reaction (Figure 4a). The current density is monitored at 0.29 V overpotential for 1 h. The value for the sharpest nanoneedles is 3 mA/cm^2 (normalized to ECSA), which is approximately 1.5 times higher than for the coarser nanoneedles and more than 3 times higher than the value measured for mixed leaf and needle structures (Figure 4b). The enhanced performance of finer needles is also apparent in CO Faradaic efficiency measurements. Sharper needles exhibit higher efficiencies for CO production at lower overpotentials (Figure 4c). At a potential of −0.4 V vs reversible hydrogen electrode (RHE), the Faradaic efficiency of CO_2 to CO conversion decreases from ∼98 to 90 and 60% as the structures become duller. This suggests that a limiting factor for achieving higher efficiencies is the availability of CO_2 molecules at the surface of electrodes.

As a result, by concentrating the electric field and subsequently by enhancing the adsorption of CO_2 molecules, not only are the reaction rates improved, but higher CO selectivity is also achieved. Although increasing the sharpness of Au needles concentrates the electric field to a greater extent, this effect is very local, and the needles' low tip radius limits the scale of the effective area (see Figure 1). We sought therefore to increase the density of active tips and took a hierarchical growth approach.

We grew the new hierarchical structures by partially covering nanoneedles using a thiol SAM and then introducing a secondary gold electrodeposition step. The SAM increases nucleation sites on the sidewalls of the nanoneedles. Without this passivation step, electrons are mostly accumulated at the

DOI: 10.1021/acs.nanolett.6b03615
Nano Lett. XXXX, XXX, XXX−XXX

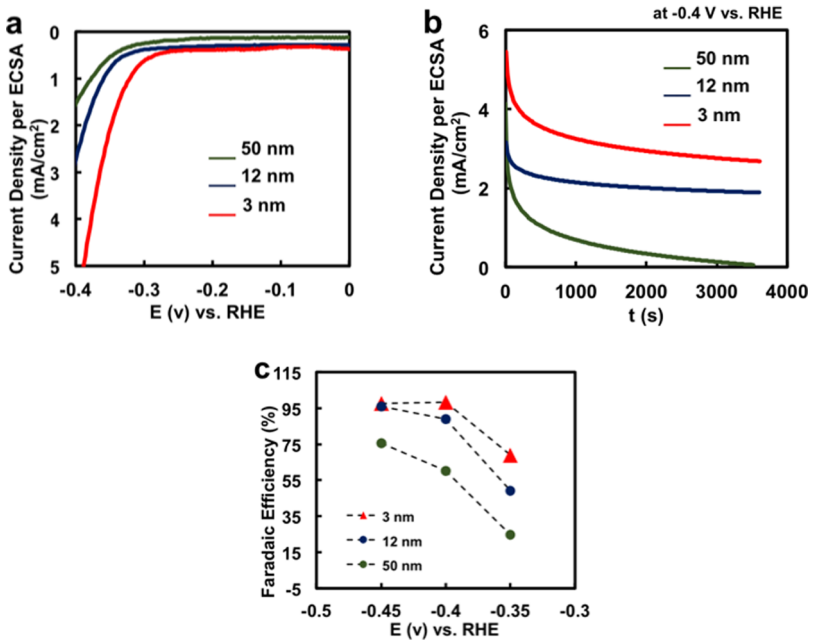

Figure 4. Sharper nanoneedles enhance the electrocatalytic performance of gold structures for CO_2 to CO reduction. (a) Partial display of cyclic voltammetry results demonstrates a higher activity of needles with lower tip radii of curvature. (b) Faster kinetics of sharper nanoneedles are evident from higher current densities obtained at −0.4 V. (c) Faradaic efficiency of generated CO using structures deposited at different overpotentials exhibit a higher efficiency of CO_2 to CO conversion achieved using sharper nanoneedles.

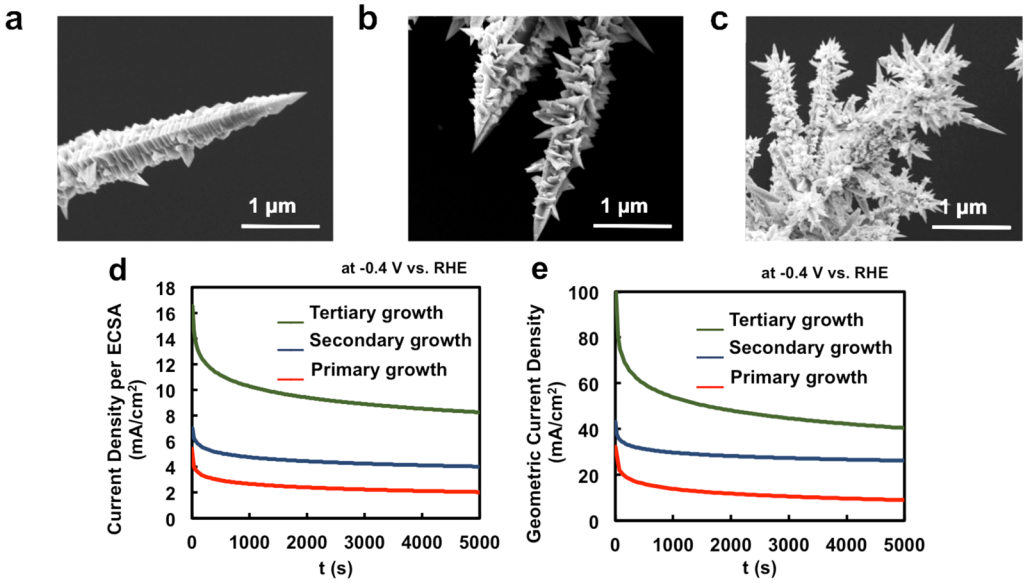

Figure 5. Structures with larger density of active sites exhibit enhanced electrocatalytic performances. SEM images showing multitip nanoneedles grown after (a) zero, (b) one, and (c) two repeat(s) of sequential thiol passivation and growth steps. (d) Current densities are enhanced, as the number of passivation-growth repeats are increased. (e) Further increase of the density of multitip structures deposited on carbon paper results in outstanding geometric current densities.

tip of the structures, and the second growth step occurs mainly at the preexisting tips (Figure S1).

When instead we apply the thiol layer, the high-energy planes and the pointed features on the sidewalls that are left uncovered become the regions of electron transfer and act as new nucleation sites. Based on this approach, we transform otherwise inactive sidewalls selectively into nucleation sites for secondary structures having active tips (Figure S2). We observe that, as each step is added in the hierarchical growth of microstructures, the number of tips is significantly increased (Figure 5a,b,c). The thiol layer was removed prior to CO_2 reduction studies, by applying 1.4 V vs Ag/AgCl electrode in 50 mM H_2SO_4 for 800 s (Figure S3).[21,22] Using these multitip Au nanoneedles for CO_2 reduction, we achieve a ECSA-normalized current density of 9 mA/cm^2 at 0.29 V overpotential, while maintaining the selectivity and achieving near quantitative CO Faradaic efficiency. The current density is about 3 times higher than that measured using single tip Au nanoneedles and 15-fold increase over the best previously reported performance (Figure 5d).[11]

DOI: 10.1021/acs.nanolett.6b03615
Nano Lett. XXXX, XXX, XXX−XXX

In practical applications, the loading of catalyst on a porous electrode to improve catalytic performance is favorable. To achieve this, we implemented the multitip Au nanoneedles on carbon fiber. As shown in Figure S2, multitip Au needles can be densely grown on carbon fiber with very sharp tips of 5 nm. The materials show a geometric current density of 38 mA/cm^2 at an overpotential of 0.29 V, which is 1.5 times higher than the best catalyst reported (Figure 5e). It should be noted that, as the number of repeats of growth-passivation steps increases, the structures become heavier; thus their mechanical stability deteriorates. This leads to the decay in current density in case of the samples developed after tertiary growth.

In summary, we demonstrate herein that sharp-tipped Au structures with smaller maximal sharpness enhance CO_2 reduction performance. We grew electrodes with optimal morphologies by promoting directional growth and increasing the fineness of gold microstructures by controlling the relative nucleation to growth rate during the electrodeposition. The Au nanoneedles with the sharpest tips (i.e., 3 nm in radii of curve) exhibit CO_2 to CO conversion with a current density per ECSA of 3 mA/cm^2, which is 5 times higher than the previously reported performance. We then further improved the performance of Au nanostructures by increasing the density of field-concentrating sites through multistep growth of secondary and tertiary pointed structures on the initially grown nanoneedles. This optimization resulted in current density per ECSA of 9 mA/cm^2 (15-fold higher than previously reported values). Finally, we leveraged our new understanding of Au nanostructure growth to maximize performance by growing multitip Au nanoneedles on porous carbon fibers. Such structures demonstrated outstandingly high geometric current densities of ~38 mA/cm^2 at 0.29 V overpotential for CO_2 reduction, proving exceptionally faster kinetics of reaction. From a broader perspective any catalyst that can be electrodeposited in the form of pointed structures can benefit from this approach to achieve more efficient and kinetically faster CO_2 electrocatalytic reduction.

■ ASSOCIATED CONTENT

Supporting Information

The Supporting Information is available free of charge on the ACS Publications website at DOI: 10.1021/acs.nanolett.6b03615.

Materials and methods (PDF)

■ AUTHOR INFORMATION

Corresponding Authors

*E-mail: shana.kelley@utoronto.ca (S.O.K.).
*E-mail: ted.sargent@utoronto.ca (E.H.S).

Funding

This work was supported by the Ontario Research Fund - Research Excellence program, the Natural Sciences and Engineering Research Council (NSERC) of Canada, the CIFAR Bio-Inspired Solar Energy program, and a University of Toronto Connaught grant.

Notes

The authors declare no competing financial interest.

■ ACKNOWLEDGMENTS

We thank Sara S. Mahshid and Sahar S. Mahshid from the University of Toronto for discussion of electrochemistry during the course of study. The authors thank Ontario Center for Characterisation of Advanced Materials (OCCAM) and Mr. Jason Tam from the University of Toronto for TEM assistance. We also acknowledge Toronto Nanofabrication Centre (TNFC) for cleanroom facilities.

■ REFERENCES

(1) Li, C. W.; Ciston, J.; Kanan, M. W. *Nature* **2014**, *508* (7497), 504−507.
(2) Rosen, B. A.; Salehi-Khojin, A.; Thorson, M. R.; Zhu, W.; Whipple, D. T.; Kenis, P. J. A.; Masel, R. I. *Science* **2011**, *334* (6056), 643−644.
(3) Qiao, J.; Liu, Y.; Hong, F.; Zhang, J. *Chem. Soc. Rev.* **2014**, *43* (2), 631−675.
(4) Lu, Q.; Rosen, J.; Zhou, Y.; Hutchings, G. S.; Kimmel, Y. C.; Chen, J. G.; Jiao, F. *Nat. Commun.* **2014**, *5*, 3242.
(5) Back, S.; Yeom, M. S.; Jung, Y. *ACS Catal.* **2015**, *5* (9), 5089−5096.
(6) Chen, Y.; Li, C. W.; Kanan, M. W. *J. Am. Chem. Soc.* **2012**, *134* (49), 19969−19972.
(7) Hori, Y. In *Modern Aspects of Electrochemistry*; Vayenas, C. G., White, R. E., Gamboa-Aldeco, M. E., Eds.; Springer: New York, 2008; pp 89−189.
(8) Raciti, D.; Livi, K. J.; Wang, C. *Nano Lett.* **2015**, *15* (10), 6829−6835.
(9) Wang, C.; Xie, Z.; deKrafft, K. E.; Lin, W. *J. Am. Chem. Soc.* **2011**, *133* (34), 13445−13454.
(10) Lin, S.; Diercks, C. S.; Zhang, Y.-B.; Kornienko, N.; Nichols, E. M.; Zhao, Y.; Paris, A. R.; Kim, D.; Yang, P.; Yaghi, O. M.; Chang, C. J. *Science* **2015**, *349* (6253), 1208−1213.
(11) Liu, M.; Pang, Y.; Zhang, B.; De Luna, P.; Voznyy, O.; Xu, J.; Zheng, X.; Dinh, C. T.; Fan, F.; Cao, C.; García de Arquer, F. P.; Safaei, T. S.; Mepham, A.; Klinkova, A.; Kumacheva, E.; Filleter, F.; Sinton, D.; Kelley, S. O.; Sargent, E. H. *Nature* **2016**, *537*, 382−386.
(12) Varela, A. S.; Kroschel, M.; Reier, T.; Strasser, P. *Catal. Today* **2016**, *260*, 8−13.
(13) Kokoszka, B.; Jarrah, N. K.; Liu, C.; Moore, D. T.; Landskron, K. *Angew. Chem.* **2014**, *126* (14), 3772−3775.
(14) Das, J.; Kelley, S. O. *Anal. Chem.* **2013**, *85* (15), 7333−7338.
(15) Lam, B.; Holmes, R. D.; Das, J.; Poudineh, M.; Sage, A.; Sargent, E. H.; Kelley, S. O. *Lab Chip* **2013**, *13* (13), 2569−2575.
(16) Mahshid, S. S.; Mepham, A. H.; Mahshid, S. S.; Burgess, I. B.; Safaei, T. S.; Sargent, E. H.; Kelley, S. O. *J. Phys. Chem. C* **2016**, *120* (37), 21123−21132.
(17) Han, J.-H.; Khoo, E.; Bai, P.; Bazant, M. Z. *Sci. Rep.* **2014**, *4*, 7056.
(18) Cogswell, D. A. *Phys. Rev. E Stat. Nonlin. Soft Matter Phys.* **2015**, *92* (1), 011301.
(19) Shao, W.; Zangari, G. *J. Phys. Chem. C* **2009**, *113* (23), 10097−10102.
(20) Lam, B.; Zhou, W.; Kelley, S. O.; Sargent, E. H. *Nat. Commun.* **2015**, *6*, 6940.
(21) Loglio, F.; Schweizer, M.; Kolb, D. M. *Langmuir* **2003**, *19*, 830−834.
(22) Yang, D. F.; Al-Maznai, H.; Morin, M. *J. Phys. Chem. B* **1997**, *101* (7), 1158−1166.

DOI: 10.1021/acs.nanolett.6b03615
Nano Lett. XXXX, XXX, XXX−XXX